

Supplementary Information for:

A New Enneanuclear Nickel(II) Cluster with a Rectangular Face-Centered Trigonal Prism Structure and Cluster Glass Behavior

Jing-Yuan Xu,^{*a} Hai-Bin Song,^b Gong-Feng Xu,^b Xin Qiao,^a Shi-Ping Yan,^{*b} Dai-Zheng Liao,^b Yves Journaux^{*c,d} and Joan Cano^e

a) School of Pharmacy, Tianjin Medical University, Tianjin 300070, China

b) College of Chemistry, Nankai University, Tianjin 300071, China

c) Institut Parisien de Chimie Moléculaire, UPMC Univ Paris 06, F-75252 Paris, France

d) CNRS UMR 7201, IPCM Paris France

e) Instituto de Ciencia Molecular (ICMol) and Fundació General de la Universitat de València (FGUV), Universitat de València, Valencia, Spain

Table of content

- | | | |
|----|---|--------------------|
| 1. | Synthesis of the complex and Structural information | S2, S3 |
| 2. | Computational details | S4, S5, S6, S7, S8 |
| 3. | Magnetic measurement | S8, S9 |

Synthesis of the complex: $[\text{Ni}(\text{ClO}_4)_2] \cdot 6\text{H}_2\text{O}$ (0.183 g, 0.5 mmol) was dissolved in methanol (10 mL), and a 20 mL methanol/water (10:1) solution of pyrazole (0.069 g, 1.0 mmol) and NaOH (0.027 g, 0.67 mmol) was added dropwise with stirring. The solution turned green with slight slurry, and stirring was maintained over 2 h at r.t. After filtering, the filtrate was subjected to one week of slow evaporation giving 32 mg of blue block single crystals suitable for X-ray diffraction, which were isolated by filtration and washed with a small amount of methanol. Yield: 36%. Elemental analysis (%) calcd for $\text{C}_{56}\text{H}_{88.5}\text{Cl}_{0.50}\text{N}_{36}\text{Ni}_9\text{O}_{23}$: C 30.85, H 4.09, N 23.31, Ni 24.23; found: C 30.86, H 3.24, N 23.21, Ni 24.55; IR (KBr pellet): $\nu = 3242$ (-OH), 1452 (C=N), 1104 cm^{-1} (ClO_4^-).

Crystal data for $[\text{Ni}_9(\mu_3-\text{OH})_6(\mu_6-\text{CO}_3)_2(\mu_2-\text{pz})_6(\text{Hpz})_{12}](\text{ClO}_4)_{0.5}(\text{OH})_{1.5}(\text{H}_2\text{O})_{7.5}$ (1): $M_r = 2180.24$, $T = 113(2)$ K, Trigonal, $R-3$ c:H, $a = b = 16.455(6)$, $c = 58.56(2)$ Å, $V = 13731(9)$ Å³, $Z = 6$, $D_{\text{calcd.}} = 1.582$ g cm⁻³, $GOF = 1.235$, $R_1 = 0.0574$, $wR_2 = 0.1443$ [$I > 2\sigma(I)$]. A total of 40952 reflections were measured in the range of $1.99^\circ \leq \theta \leq 27.88^\circ$, and 3648 [$R(\text{int}) = 0.0585$] unique reflections with $I > 2\sigma(I)$ were used in the succeeding refinements. Data collection, structure solution and refinement used programs Crystalclear, SHELXS-97 and SHELXL-97. Full details have been deposited and will be published later. CCDC 644657.

Nitrate was not present in the reaction at any stage; therefore it appears that atmospheric CO₂ has been incorporated into the crystal structure reasonably owing to the basic media afforded by the addition of NaOH.

Table S1. Selected bond lengths [Å] and angles [°] for complex 1.

Ni(1)-N(5)#1	2.050(2)	Ni(2)-N(3)	2.0944(18)
Ni(1)-N(5)	2.050(2)	Ni(2)-N(1)	2.099(2)
Ni(1)-O(1)#1	2.0514(15)	Ni(2)-O(1)	2.1090(17)
Ni(1)-O(1)	2.0514(15)	Ni(2)-O(2)#1	2.1671(16)
Ni(1)-O(2)#1	2.1625(15)	O(1)-Ni(2)#2	2.0387(17)
Ni(1)-O(2)	2.1627(15)	O(2)-Ni(2)#1	2.1671(16)
Ni(2)-O(1)#2	2.0387(17)	N(6)-Ni(2)#1	2.0674(18)
Ni(2)-N(6)#1	2.0675(18)		
N(5)#1-Ni(1)-N(5)	101.69(11)	O(1)#2-Ni(2)-N(6)#1	167.60(7)
N(5)#1-Ni(1)-O(1)#1	97.81(6)	O(1)#2-Ni(2)-N(3)	92.42(7)
N(5)-Ni(1)-O(1)#1	86.72(6)	N(6)#1-Ni(2)-N(3)	91.78(8)
N(5)#1-Ni(1)-O(1)	86.72(6)	O(1)#2-Ni(2)-N(1)	95.95(8)
N(5)-Ni(1)-O(1)	97.81(7)	N(6)#1-Ni(2)-N(1)	95.66(9)
O(1)#1-Ni(1)-O(1)	172.85(9)	N(3)-Ni(2)-N(1)	90.63(7)
N(5)#1-Ni(1)-O(2)#1	86.29(7)	O(1)#2-Ni(2)-O(1)	81.07(7)
N(5)-Ni(1)-O(2)#1	171.88(7)	N(6)#1-Ni(2)-O(1)	86.72(7)
O(1)#1-Ni(1)-O(2)#1	93.74(5)	N(3)-Ni(2)-O(1)	99.88(7)
O(1)-Ni(1)-O(2)#1	80.99(6)	N(1)-Ni(2)-O(1)	169.16(6)
N(5)#1-Ni(1)-O(2)	171.89(7)	O(1)#2-Ni(2)-O(2)#1	91.80(5)
N(5)-Ni(1)-O(2)	86.29(7)	N(6)#1-Ni(2)-O(2)#1	83.85(6)
O(1)#1-Ni(1)-O(2)	80.99(6)	N(3)-Ni(2)-O(2)#1	175.62(7)
O(1)-Ni(1)-O(2)	93.74(5)	N(1)-Ni(2)-O(2)#1	90.11(6)
O(2)#1-Ni(1)-O(2)	85.78(8)	O(1)-Ni(2)-O(2)#1	79.61(5)

Symmetry transformations used to generate equivalent atoms:

#1 x-y+1/3,-y+2/3,-z+1/6 #2 y+1/3,x-1/3,-z+1/6 #3 -x+y+1,-x+1,z
#4 -y+1,x-y,z #5 -y,x-y,z #6 -x+y,-x,z

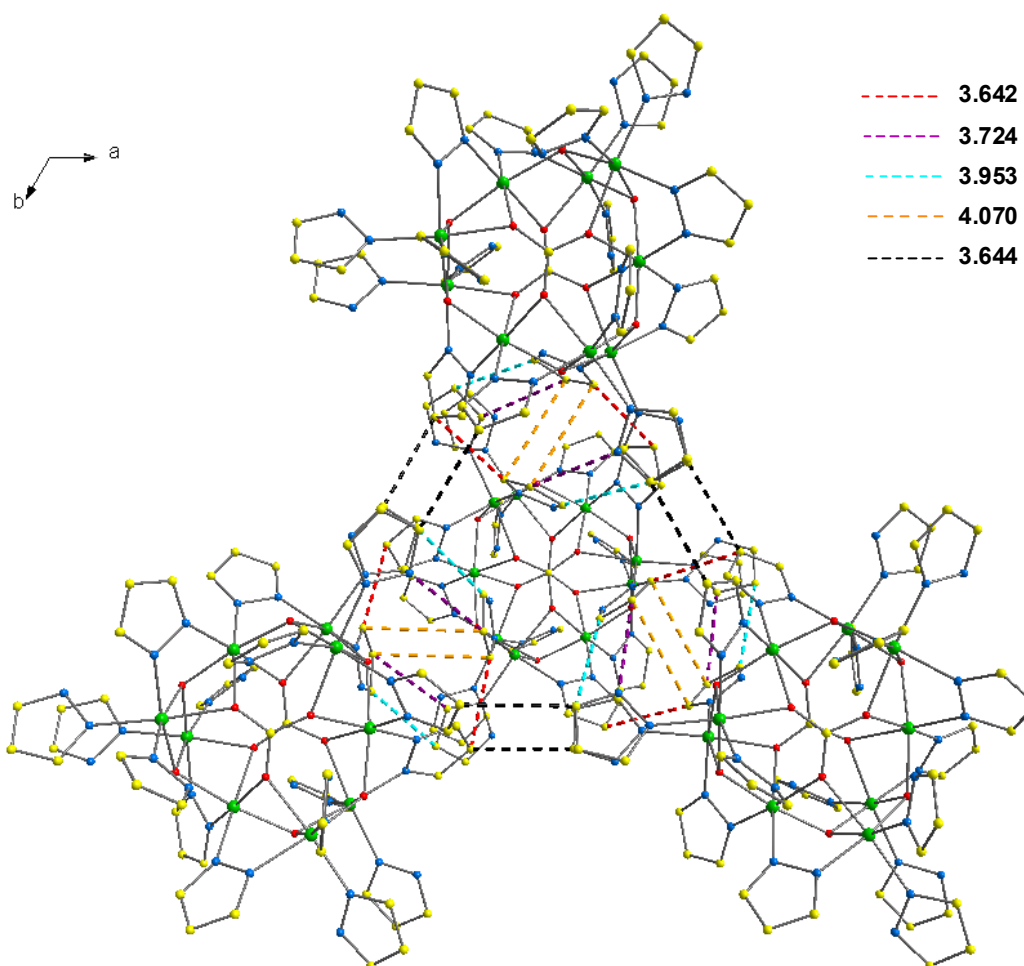


Figure S1. Packing plot of complex 1 viewed along *c*-axis, showing various π - π interactions between the pyrazolate groups from the neighboring clusters with interplanar distance (\AA) in colorful dashed lines. H atoms, uncoordinated perchlorate and hydroxyl anions were omitted for clarity.

Computational Details

In our calculations, we employed the experimental structures that take into account small variations in the geometry induced by intermolecular interactions that may result in large changes in the calculated exchange coupling constants due to the strong dependence of the magnetic properties with structural parameters. Calculations with the B3LYP functional¹ were performed with NWChem code^{2,3} using the quadratic convergence approach and a guess function generated with the Jaguar 6.5 code.⁴ The triple- ζ all electron Gaussian basis set proposed by Schaefer *et al.* was employed.⁵

Discussion

Theoretical methods based on density functional theory have been extensively employed since some time ago to study the spin states from simple molecules⁶ to polynuclear metal clusters.⁷ Such methodology also allows to obtain all the exchange coupling constants that are present in polynuclear transition metal complexes.^{8,9} In order to calculate the $n J_i$ exchange coupling constants of a polynuclear complex, we must at least perform $n+1$ energy calculations of different spin configurations that correspond to single-determinant Kohn-Sham solutions.⁸ Such spin configurations must be selected in such way that it is possible to solve a system of n equations with n unknowns, the J values. However, in order to minimize the effects of a low symmetry or, even, a dependence of the calculated J values on the selected set of spin configurations, we have chosen some extra confirmations. This procedure allow us to discern the presence of non-negligible interactions between the second neighbours or some dependence of the configurations on our results as well as to obtain a more accurate estimation for the mean value of the exchange coupling constants and to validate the approaches that have been considered in the topology of magnetic interactions. In this way, eleven calculations were performed on the Ni₈ complex in order to obtain the two exchange coupling constants by least-squares fitting for the following spin configurations: a high spin ($S = 9$) that provide the reference in energy, one $S = 5$ (<{Ni1, Ni3}), six $S = 3$ (<{Ni1, Ni2, Ni7}, {Ni3, Ni6, Ni9}, {Ni1, Ni2, Ni3}, {Ni1, Ni3, Ni5}, {Ni1, Ni3, Ni9} and {Ni2, Ni5, Ni8}) and three $S=1$ (<{Ni1, Ni2, Ni3, Ni9} and {Ni3, Ni4, Ni7, Ni8})) spin distributions, where only the spin-down centers are indicated in the notation used here, which is shown in Figure S2. These spin distributions and the relative energies as a function of the magnetic coupling constants (J) are given in Table S2.

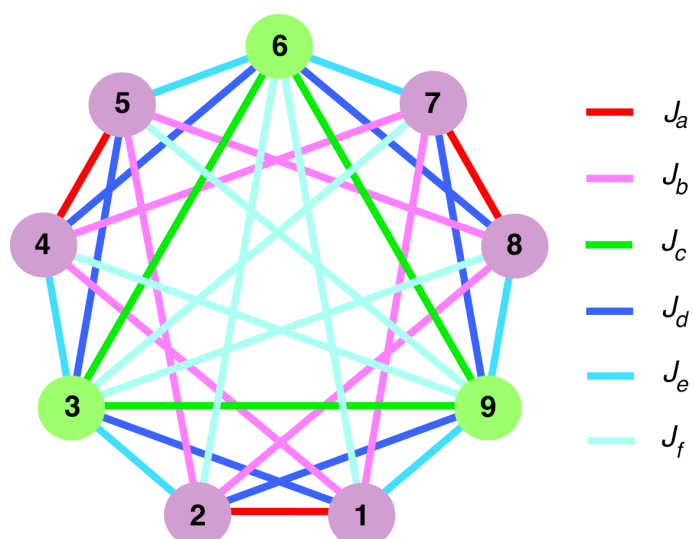


Figure S2. Scheme showing the topology of the spin-spin exchange interactions in complex 1

According to the description of the structure in the manuscript and the different pathway involved in the magnetic couplings (see text in the manuscript), six different exchange interactions have been considered in Ni₉ complex. Actually, more exchange couplings can be considered due to the low symmetry of the complex; however, since small changes in the geometrical parameters we have preferred to use a simple topology of the magnetic interaction with only one value for J_b and one for J_c (structural differences of 0.001 Å and 0.002 Å, respectively, in the metal-metal distances). That is why, an average values is found for these two magnetic coupling constants. An analysis of the validity of this approach has been done in our theoretical study. In this situation, the considered spin Hamiltonian can be expressed as follows:

$$\begin{aligned}\hat{H} = & -J_a(\hat{S}_1\hat{S}_2 + \hat{S}_4\hat{S}_5 + \hat{S}_7\hat{S}_8) - J_b(\hat{S}_1\hat{S}_4 + \hat{S}_2\hat{S}_5 + \hat{S}_4\hat{S}_7 + \hat{S}_5\hat{S}_8 + \hat{S}_1\hat{S}_7 + \hat{S}_2\hat{S}_8) \\ & - J_c(\hat{S}_3\hat{S}_6 + \hat{S}_3\hat{S}_9 + \hat{S}_6\hat{S}_9) - J_d(\hat{S}_1\hat{S}_3 + \hat{S}_3\hat{S}_5 + \hat{S}_2\hat{S}_9 + \hat{S}_7\hat{S}_9 + \hat{S}_4\hat{S}_6 + \hat{S}_6\hat{S}_8) \\ & - J_e(\hat{S}_2\hat{S}_3 + \hat{S}_3\hat{S}_4 + \hat{S}_5\hat{S}_6 + \hat{S}_6\hat{S}_7 + \hat{S}_1\hat{S}_9 + \hat{S}_8\hat{S}_9) - J_f(\hat{S}_1\hat{S}_6 + \hat{S}_2\hat{S}_6 + \hat{S}_3\hat{S}_7 + \hat{S}_3\hat{S}_8 + \hat{S}_4\hat{S}_9 + \hat{S}_5\hat{S}_9)\end{aligned}\quad (\text{Eq. 1})$$

where S_i are the local spin operators of each paramagnetic center. The results obtained for J_{a-f} using ten equations from eleven different spin distributions (Table S2) are displayed in Table S3. The found standard deviations are small and in agreement with the used approaches. Therefore, the addition of new exchange couplings between the closest second neighbours is absolutely unnecessary. Additional calculations have been done to calculate the different J constants in an individual way. For it, nickel(II) ions have been replaced by non-magnetic zinc(II) ions and only those nickel centres that are involved in a certain magnetic coupling have been preserved. For all cases, the J values have been estimated from the calculated quintuplet and singulet spin states. The results are also displayed in Table S3. These results are in agreement with the previous ones obtained for the real Ni₉ molecule and also a slight shift to the antiferromagnetic regions that is observed in all J constants and that, probably, is due to small changes in the electronic structure introduced by the zinc(II) ions. Moreover, from the previous study in dinuclear complexes where only one atom make up the exchange pathway, the small or moderate variations considered for the exchange coupling constants can be reproduced by small changes in some geometrical parameters such as the NiONi angle.^{8a,9a} Thus, whereas large values of the NiONi angle induces strong antiferromagnetic coupling (J_d), small values leads to weak ferromagnetic coupling (J_a and J_e). May be, the antiferromagnetic contribution in J_d is even reduced by an orbital counter-complementary effect roused by the combined presence of the carbonate and hydroxo bridging ligands, but without being counterbalanced by the ferromagnetic contribution. Moreover, such as it is expected, a stronger antiferromagnetic coupling is observed in the case where the carbonate is coordinated in an anti-anti conformation (J_f), leading to a weak antiferromagnetic or even ferromagnetic coupling when the syn-anti conformation (J_b and J_c) is presented. On the other hand, we can conclude that the moderate standard deviations are connected to the process of the modelization by increasing of the molecular symmetry.

Table S2. Calculated broken-symmetry configurations and relative energies as a function of exchange coupling constants. In the spin configuration, is noted only with spin-down centers.

State	Spin configuration	J_a	J_b	J_c	J_d	J_e	J_f
ST1	{Ni1, Ni4, Ni7}	9	0	0	9	9	9
ST2	{Ni3, Ni6, Ni9}	0	0	0	18	18	18
ST3	{Ni1, Ni2, Ni3}	0	12	6	6	6	12
ST4	{Ni1, Ni2, Ni3, Ni9}	0	12	6	6	6	18
ST5	{Ni6, Ni7, Ni8, Ni9}	0	12	6	6	6	18
ST6	{Ni1, Ni3, Ni5}	6	12	6	0	12	12
ST7	{Ni1, Ni3, Ni9}	3	6	6	9	9	15
ST8	{Ni1, Ni3}	3	6	6	3	9	9
ST9	{Ni3, Ni4, Ni7, Ni8}	3	12	6	15	9	3
ST10	{Ni2, Ni5, Ni8}	9	0	0	9	9	9

Table S3. Magnetic exchange coupling (J_i), bridging ligands (L_i), selected structural parameters (in Å and in deg) and theoretical and experimental magnetic coupling constants (in cm^{-1}) for **1**.

J_i	Sites {i,j}	$d_{M\text{-}M}/\text{\AA}$	L_i	$d_{M\text{-}Li}/\text{\AA}$	$d_{M\text{-}Li}/\text{\AA}$	$\mathbf{M}\text{-}\mathbf{L}\text{-}\mathbf{M}^o$	J_{DFT} ^a	$J_{\text{DFT(2)}}$ ^b	J_{exp}
J_a	{1, 2} ^c	3.142	$\int_{_3\text{-OH}}$	2.038	2.110	98.5	+0.95 (0.17)	+4.7	+0.6
			$\int_{_3\text{-OH}}$	2.110	2.038	98.5			
J_b	{1, 4} ^d	5.569	$\int_{_2\text{-CO}_3}{}^i$	2.168	2.167	----	+0.8 (0.3)	+0.7	+0.6
			$\int_{_3\text{-CO}_3}{}^i$	2.165	2.165	----	-1.7 (0.5)	-1.5	+1.5
J_c	{3, 6} ^e	4.793	$\int_{_3\text{-CO}_3}{}^i$	2.162	2.162	----			
			$\int_{_3\text{-OH}}$	2.038	2.052	128.0	-29.06 (0.14)	-27.7	-27.5
J_d	{1, 3} ^f	3.677	$\int_{_2\text{-CO}_3}{}^j$	2.168	2.161	----			
			$\int_{_3\text{-OH}}$	2.110	2.052	95.0			
J_e	{2, 3} ^g	3.069	$\int_{_2\text{-OCO}_2}$	2.168	2.165	90.2	+1.53 (0.21)	+3.0	+0.6
			$\int_{_2\text{-pZ}}$	2.068	2.052	----			
J_f	{1, 6} ^h	6.158	$\int_{_2\text{-CO}_3}{}^k$	2.168	2.162	----	-4.34 (0.12)	-4.2	-6.9

^a from {Ni₉} molecule an standard deviation in parentheses, ^b from {Ni₂Zn₇} molecules ^c {1,2}, {4,5},{7,8}, ^d {1,4}, {1,7},{4,7},{2,5}, {2,8},{5,8}, ^e {3,6}, {3,9}, {6,9}, ^f {1,3}, {3,5}, {2,9}, {7,9}, {4,6}, {5,6}, {6,8}, ^g {2,3}, {3,4}, {6,7}, {1,9}, {8,9}, ^h {1,6}, {2,6}, {3,7}, {3,8}, {4,9}, {5,9}, ⁱ, ^j syn-syn conformation, ^j anti-anti conformation

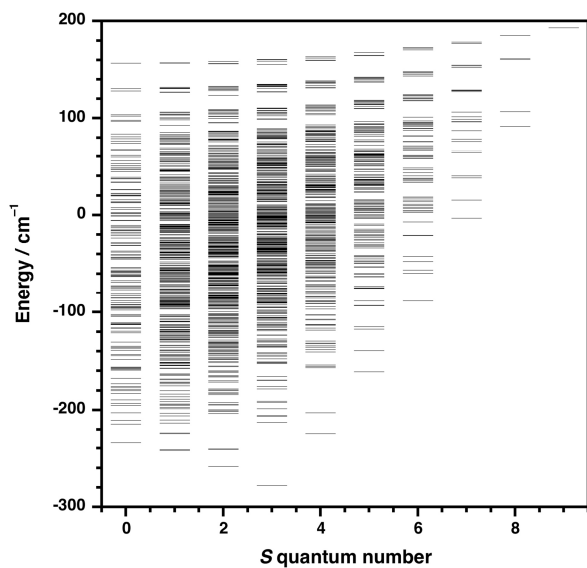


Figure S3. Energy spectra of quantum spin S for **1** calculated from the J values found in the fit of the magnetic susceptibility data.

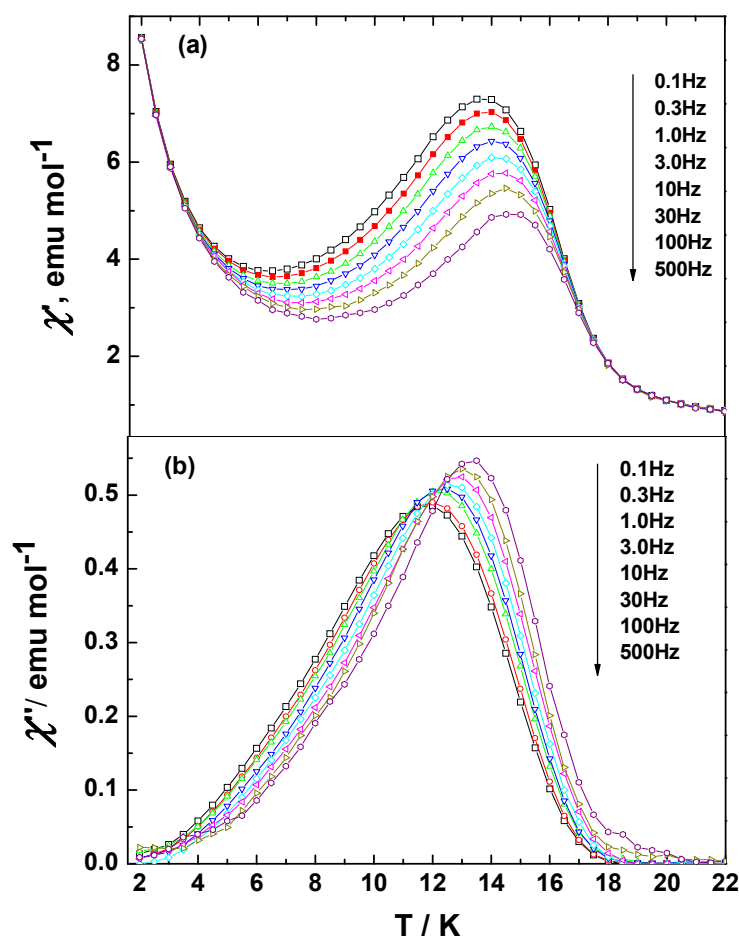


Figure S4. Temperature and frequency dependence of (a) real (χ') and (b) imaginary (χ'') parts of the ac susceptibility ($H_{dc} = 0$ Oe, $H_{ac} = 1$ Oe) for complex **1**.

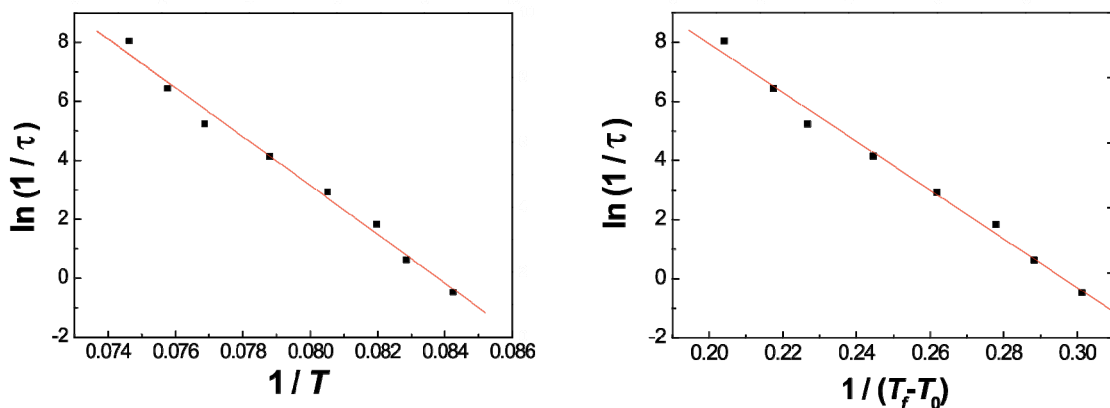


Figure S5. Relation between the frequency of the measurement (v , in Hertz), and the blocking temperature (T_f) with a best-fit to Arrhenius expression (left) and the Vogel-Fulcher law (right).

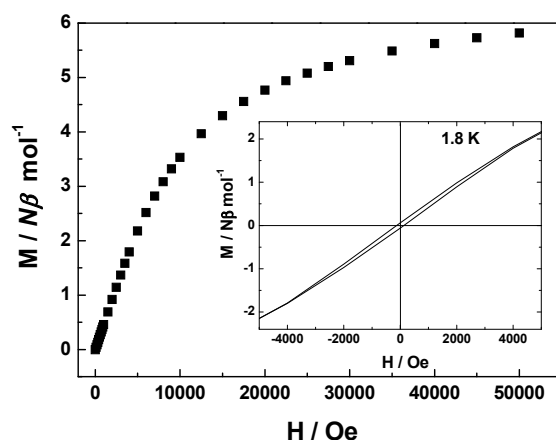


Figure S6. Field dependence of the magnetization at 1.8 K for **1**. Insert: hysteresis loop ($M/N\beta$ vs H) at 1.8 K.

References

- 1) Becke, A. D. *J. Chem. Phys.* **1993**, *98*, 5648-5652.
- 2) Aprà, E. et al. NWChem 4.7 Richland, Washington , 2005
- 3) Kendall, R. A.; Aprà, E.; Bernholdt, D. E.; Bylaska, E. J.; Dupuis, M.; Fann, G. I.; Harrison, R. J.; Ju, J. L.; Nichols, J. A.; Nieplocha, J.; Straatsma, T. P.; Windus, T. L.; Wong, A. T. *Comp. Phys. Comm.* **2000**, *128*, 260.
- 4) Jaguar 6.0; Schrödinger, Inc.: Portland, 2005.
- 5) Schaefer, A.; Huber, C.; Ahlrichs, R. *J. Chem. Phys.* **1994**, *100*, 5829-5835.
- 6) Goursot, A.; Malrieu, J. P.; Salahub, D. R., *Theor. Chim. Acta* **1995**, *91*, 225.
- 7) Castro, M.; Salahub, D. R., *Phys. Rev. B* **1993**, *47*, 10955.
- 8) (a) Ruiz, E.; Alemany, P.; Alvarez, S.; Cano, J. *J. Am. Chem. Soc.* **1997**, *119*, 1297-1303 (b) Ruiz, E.; Cano, J.; Alvarez, S.; Alemany, P., *J. Comp. Chem.* **1999**, *20*, 1391. (c) Ruiz, E.; Rodríguez-Fortea, A.; Cano, J.; Alvarez, S.; Alemany, P., *J. Comp. Chem.* **2003**, *24*, 982. (d) Ruiz, E.; Alvarez, S.; Cano, J.; Polo, V. *J. Chem. Phys.* **2005**, *123*, 164110
- 9) (a) Ruiz, E.; Cano, J.; Alvarez, S.; Alemany, P. *J. Am. Chem. Soc.* **1998**, *120*, 11122. (b) Ruiz, E.; Cano, J.; Alvarez, S.; Caneschi, A.; Gatteschi, D., *J. Am. Chem. Soc.* **2003**, *125*, 6791.
- 10) Cano, J.; Costa, R.; Alvarez, S.; Ruiz, E. *J. Chem. Theory Comput.* **2007**, *3*, 782.